# Verification of the Nucleation of Pyramidal Structures during Sputtering of Clean Germanium (110) Crystals

Hazel Betz, Oregon State University

## Abstract

The nucleation of pyramidal structures on the surface of germanium (110) after the Ge was sputtered with argon ions was first observed by a previous graduate student in the Chiang Group, Marshall van Zijll. The structures were approximately 100 nm across, and their formation was initially attributed solely to the sputtering process. A question was raised about possible contamination on van Zijll's samples due to traces of silver that may have been on the sample holders. We attempted to re-create one of van Zijll's experiments with an uncontaminated sample holder. No results were achieved due to numerous technical setbacks. However, much work was done to troubleshoot and fix the scanning tunneling microscope used in the experiments.

## Introduction

The Chiang Group explores the surface physics of metals and semiconductors in ultrahigh vacuum (UHV) conditions. Ultrahigh vacuum, the pressure regime below $10^{-10}$ torr, is necessary to maintain the surface cleanliness of samples being studied. A unique laboratory setup consisting of a scanning tunneling microscope (STM), a low energy electron microscope (LEEM), and an x-ray photoemission spectrometer (XPS) are all contained in a single UHV system. This allows a single sample to be analyzed in all three machines without causing sample contamination by breaking vacuum. Figure 1 gives a schematic overview of the laboratory apparatus.

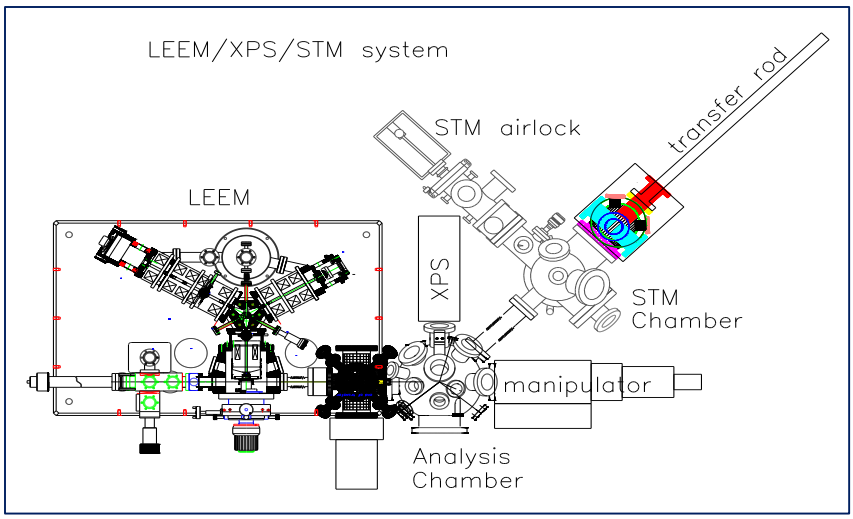


**Figure 1.** The laboratory has 3 complementary instruments (STM, LEEM, and XPS) in interconnected UHV chambers that allow sample exchange without breaking vacuum. [1]

During my time in Dr Chiang's laboratory, I worked closely with graduate student Andrew Kim. We attempted to use the STM to confirm results found by a previous Chiang Group graduate student, Marshall van Zijll. He had observed pyramidal structures forming on the surface of germanium (110) crystals when the Ge was sputtered with argon ions as part of a standard cleaning process. In van Zijll's experiments, different sputtering energies led to pyramids of different sizes and geometries, one example of which is shown in Figure 2.

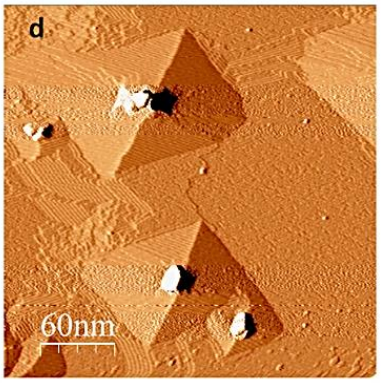


**Figure 2.** Pyramidal structures approximately 100 nm wide observed by van Zijll on germanium (110) after sputtering [1]

However, it was possible that the sample holders used in van Zijll's experiments characterizing these pyramidal structures were contaminated with traces of silver. In a previous set of experiments, van Zijll had used the same sample holders while depositing evaporated silver onto the surface of his samples. Though it is possible that the traces of silver present on the sample holders could have contaminated the clean germanium samples during the sputtering process and caused the nucleation of the pyramids.

The following sections details the steps and setbacks that were encountered while attempting to determine whether van Zijll's observed pyramids were a direct result of sputtering the surface of clean germanium (110) or were nucleated due to silver contamination.

## Background

Much past research has been done to understand the response of materials when they are sputtered. Sputtering is known to cause a variety of surface modifications on different materials including structural, topographical, electronic, and compositional changes [2]. Sputtering techniques are used in many applications, including spectroscopy, advanced ceramics, and integrated circuits [2]. Although the pyramids characterized by van Zijll are primarily of interest as semi-ordered defects, the topographic changes observed on Ge(110) could have possible applications. For example, if the parameters controlling the nucleation and growth of these pyramidal structures were fully understood, a controlled pyramidal pattern could be constructed by forming a pattern of nucleation points and then sputtering the surface [1].

## Sample Holders

The laboratory's sample holders both hold the samples being studied and contain a small tungsten filament that allows the sample to be heated in the cleaning processes and during experimentation.

Figure 3 displays the top and bottom of the sample holder as well as an exploded view showing the holder's different components. All of the components in the sample holder used for re-creating van Zijll's experiments were new in order to rule out possible contamination from previous experiments.

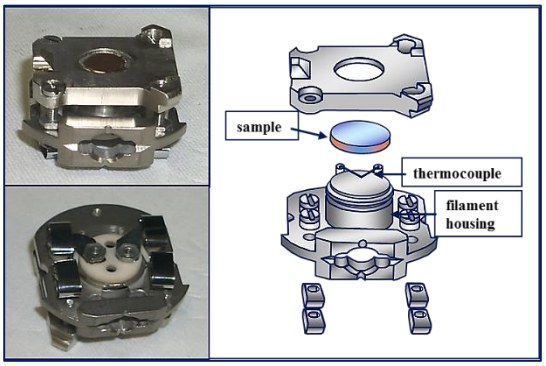


**Figure 3.** Three-quarter view of top and bottom of sample holder with additional exploded view [1].

## Cleaning Samples

Van Zijll noticed small pyramidal structures forming on the surface of Ge(110) samples during the laboratory's routine cleaning process [1]. When a new sample enters the laboratory's ultrahigh vacuum system, it must be cleaned through a combined process of sputtering and annealing. This removes the inevitable contamination on the surface of the sample due to previous atmospheric exposure. However, the sputtering step in this cleaning process is also what may have produced the pyramids on the surface of the Ge (110) samples.

A single cycle of the cleaning process used on the Ge (110) requires two steps. The sample is first sputtered for 15 minutes. Argon ions are accelerated by an electric field and hit the surface of the sample with an energy of 400 keV. These collisions remove atoms from the surface of the sample, thereby removing contaminants, but sputtering also roughens the surface of the sample considerably. The sample is then annealed for 10 minutes. During annealing, the sample is heated to 800°C, to allow the top atomic layers of the surface to recrystallize, making the surface smooth again. The annealing temperature is chosen to be below 938° C, the melting point of bulk Ge, so as not to melt the sample and destroy the crystal lattice structure.

In order to achieve a clean sample, between 12 and 16 cleaning cycles are typically required. However, the pyramidal structures that van Zijll observed were seen to form after as few as six cleaning cycles and to become more pronounced as more cleaning cycles were performed [1]. To confirm van Zijll's observations, a clean Ge (110) sample was to be placed into a previously unused sample holder, and observations were to be made after 6, 14, 21, and 32 cycles of cleaning. Figure 4 shows the STM scans of van Zijll's pyramidal structures during the experiment that we were attempting to re-create.

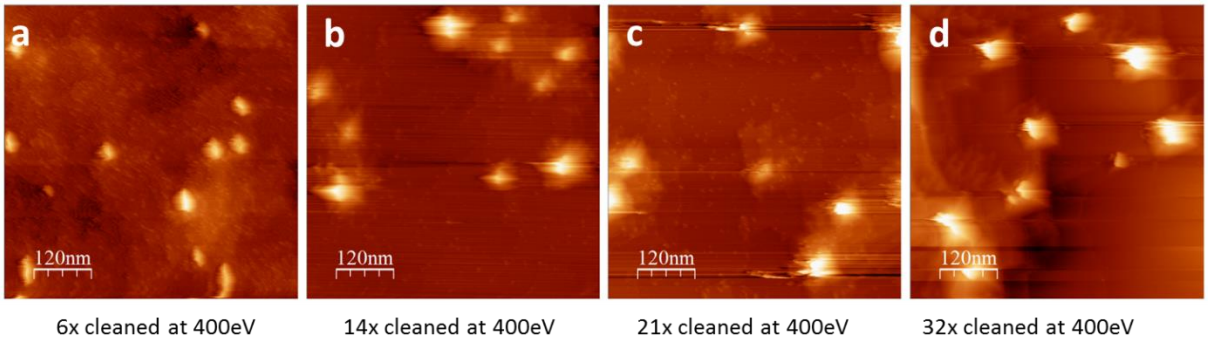


**Figure 4.** The pyramidal formations that van Zijll observed on Ge (110) got progressively larger and more defined as more sputtering cycles were performed on the sample. These STM images were taken after a) six cleaning cycles, b) 14 cleaning cycles, c) 21 cleaning cycles, d) 32 cleaning cycles. Our goal was to re-create this experiment with a clean sample holder. [1]

## Scanning Tunneling Microscope

A scanning tunneling microscope (STM) can achieve atomic resolution by using the quantum tunneling of electrons to image the surface of the sample. As seen in Figure 5, the scanning tip of an STM is a very thin piece of metal, ideally only a single atom wide, that is brought within several nanometers of the surface of a sample. A bias voltage is applied between the tip and the sample, allowing electrons to tunnel through the forbidden region between them and create a small current that can be detected with sensitive instrumentation [4]. Equation 1 gives the equation governing the tunneling current

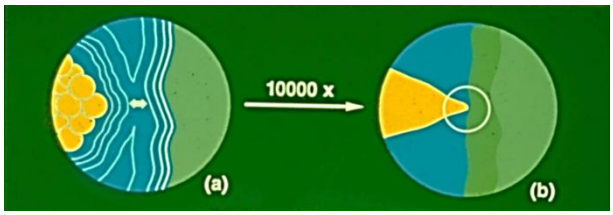


**Figure 5.** a) Tip of the STM a few nanometers away from the surface of the sample allowing electrons to tunnel between them. b) Shows 10000x zoomed out perspective [3]

$$I = Ve^{-A\sqrt{\Phi}z} \quad [1]$$

where I is current, V is voltage, A is a constant, Φ is the average work function of tip and sample, and z is the separation of tip and sample [5].

To allow an STM to record topographic data in the laboratory, a feedback loop is used to maintain a constant tunneling current, usually 2 nA. This constant tunneling current is maintained by moving the tip of the STM up and down as it scans laterally across the surface of a sample. By recording the tip's height during its numerous passes across the sample, a topographic image of the sample's surface can be collected by the computer.

## Mechanical Overview of the STM

Figure 6 shows the mechanical components of the Chiang laboratory's STM. Highlighted in red is the STM scanner that holds the scanning tip. When a new scanning tip is required, this scanner is removed from the UHV system, a new tip is mounted, and the scanner is returned to the system. Because of the STM's extreme sensitivity to vibration, during scans the entire high vacuum system containing the STM chamber is floated on pneumatic isolators of the type commonly used to support laser tables. In addition, the platform supporting the scanner is

suspended on springs, and permanent magnets near copper supports damp the spring vibrations via eddy currents.

**Figure 6.** The mechanical setup of the STM inside the vacuum chamber. The scanner, shown in red, can be removed from the chamber to allow tip replacements. A sample holder can be seen below the scanner, although the scanner's tip is too small to be visible. [1]

## Repairing the STM Scanner

Before the project could begin, one of the STM scanners needed to be repaired. The metal tube used to mount the STM's scanning tip broke, requiring the scanner head to be disassembled. Once the scanner head was dissembled, a new mounting tube was secured to the piezoelectric cylinder that controlled the fine x, y, and z motions of the scanning tip near the sample surface. The new mounting tube was then electrically reconnected to the scanner with a new coaxial cable.

Because many materials have too high a vapor pressure to be used in a UHV system, special silver paste and "Torr Seal" epoxy were used to replace the mounting tube and attach the new coaxial cable to the head of the scanner. The other end of the coaxial cable was soldered with high vacuum solder and a separate acid flux so that the flux could be removed by washing the joint with de-ionized water before putting the scanner back into the UHV system. Figure 7 shows the scanner in three different stages of repair.

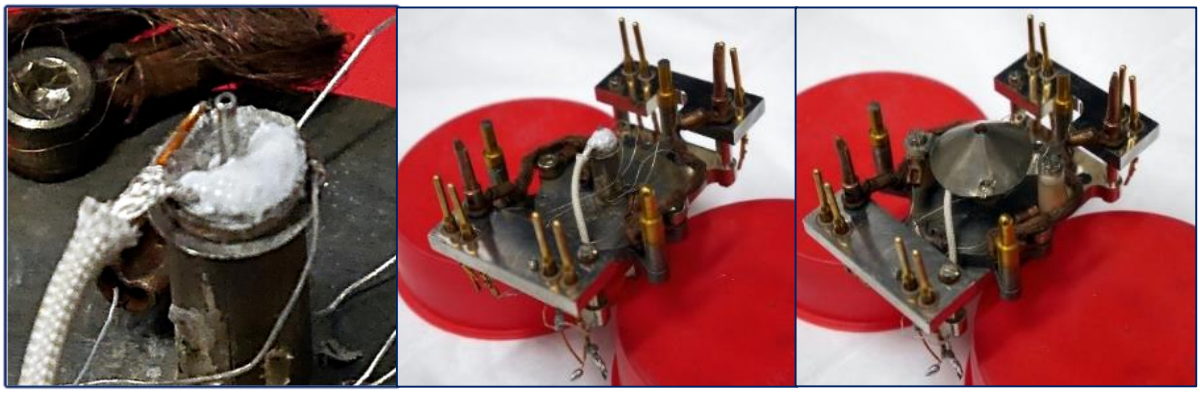

**Figure 7.** The STM scanner head in different stages of repair. Left, a close-up of the disassembled scanner head showing the new tube and coaxial cable. Center, the scanner with the ends of a new coaxial cable secured with UHV compatible solder on one end, and silver paste and Torr Seal on the other. Right, the fully repaired scanner.

## Making STM Tips

In addition to repairing one of the scanners, new scanning tips had to be manufactured for the STM. Figure 8 shows the laboratory setup for tip production. Scanning tips for the STM were made out of tungsten wire etched in an electrochemical reaction using a 3M solution of potassium hydroxide (KOH). On one side of a custom glass cell, the tip of a tungsten wire was submerged just below the surface of the KOH. The other end of the tungsten wire was connected to a DC power source. On the other side of the glass cell, a copper anode was also connected to the DC power source completing a circuit that ran through the KOH solution. Once the circuit through the solution was complete, a small current starting around 25 mA was applied. This current immediately began decreasing as the tungsten wire was etched away.

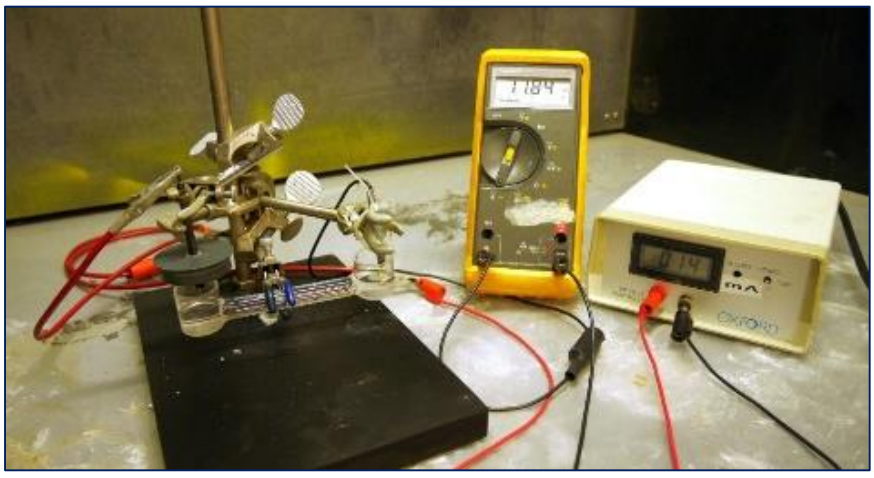

**Figure 8.** STM tips are etched in a DC electrochemical reaction using potassium hydroxide. The meniscus of the KOH solution etches the tungsten wire into a sharp tip.

During the electrochemical reaction, the meniscus on the KOH caused uneven etching of the tungsten wire. The tungsten wire at the meniscus etched more quickly than the wire in the main solution. This caused the length of tungsten wire below the meniscus to drop off when the tungsten wire at the meniscus etched through. This uneven etching produced a highly tapered tip on the end of the wire

The power source was programmed to shut off when the current fell below 5 mA, corresponding to the "drop off" of the wire below the meniscus. This prevented further etching that might dull the tip formed on the wire.

Because the surface effects at the meniscus of the KOH produced the sharp tip on the tungsten wire, the experimental setup for tip manufacturing needed to be closely protected from drafts that could disturb the level of the meniscus on the wire while it was etching. Figure 9 shows both a well etched tip and a badly etched tip as seen through an optical microscope with 20x magnification. The badly formed tip on the right is probably due to drafts disturbing the level of the meniscus of the KOH solution during the etching process.

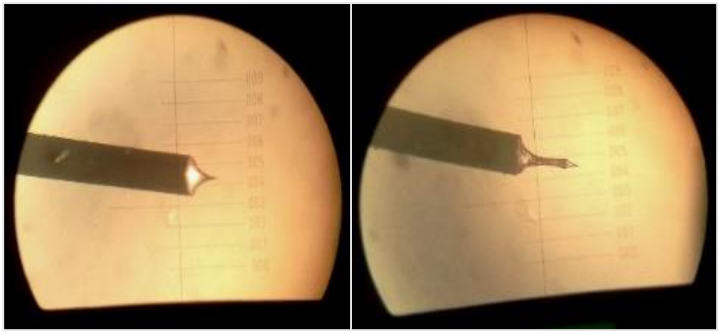

**Figure 9.** The left photograph shows a well etched STM tip with the tungsten wire ending in a short sharp point. The right shows a badly etched STM tip with the tungsten wire ending in a long irregular point, likely due to drafts changing the level of the KOH meniscus during etching.

After the new STM tips were made, the correct tip mounting height had to be found through trial and error on the repaired scanner. Figure 10 gives a side view of the STM scanner showing where tips were mounted. If the tip was too high, it would not reach the surface of the sample, and if the tip was too low, it would immediately "crash" on the surface of the sample. In both of these cases, a successful scan would be impossible. After several attempts, the correct height for mounting tips on the repaired scanner was found, and a successful test scan was done with the repaired scanner.

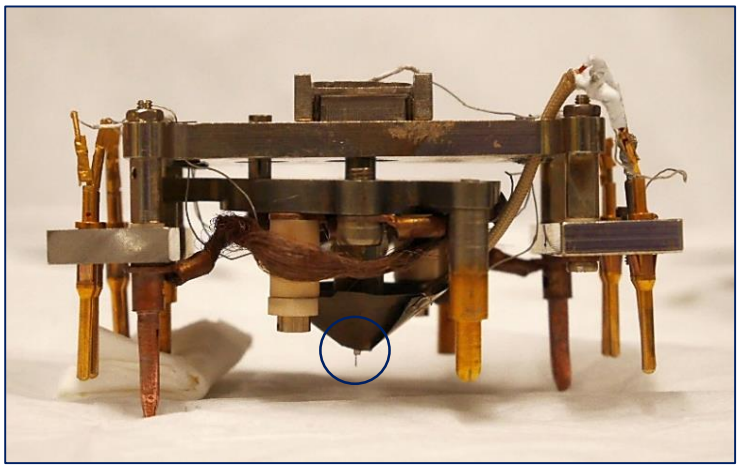

**Figure 10.** A side view of the STM scanner with the blue circle showing the location of mounted scanning tip. There was a 1 mm window in which STM tips could be mounted for a successful scan. If the tip was too high, it would not reach the sample, and if it was too low, it would crash onto the sample.

## Repairing the STM Chamber Piezoelectric Elements

After the STM scanner had been fixed, new tips had been made, and the new scanning tip height had been found, the piezoelectric components for coarse motions of the tip with respect to the sample in the STM chamber stopped working. Piezoelectric materials generate an internal voltage in response to an applied mechanical stress, and conversely, apply mechanical stress to their surroundings in response to an applied voltage. Piezoelectric elements are commonly used to control motion in STMs, because the application of voltage across them can be calibrated to produce the highly controlled and precise movements necessary for STM function.

Two "Z" piezoelectric elements in the laboratory's STM chamber were used to control the initial approach of the tip to the sample and two "X" piezoelectric elements were used to control lateral movement of the tip. These Z and X piezoelectric elements were controlled through four different channels: forward Z, reverse Z, forward X, and reverse X. It appeared that all four of these channels had stopped working.

After troubleshooting, it was discovered that there was a broken wire and a faulty switch in the control box for the chamber piezoelectric elements and a loose connector on one of the coaxial cables. When these were fixed, both of the X piezoelectric elements functioned, but the Z elements still did not.

Upon further investigation, an error was discovered in the signals being sent to the piezoelectric elements in the STM chamber. All four channels were supposed to receive the same voltage signal, a repeated linear pulse that increased by 400 V over 2 ms, when the channel was engaged.

The voltage was simply reversed across the piezoelectric elements connected to the reverse Z and reverse X channels. However, Table 1 shows the logic error that was discovered. Both the forward and reverse X piezoelectric channels were working correctly, but both the forward and reverse Z piezoelectric channels sent a signal to the forward piezoelectric channels for both the X and the Z.

| | |
|---|---|
| A1 channel | signal sent to move X backward |
| A2 channel | signal sent to move X forward |
| B1 channel | signal sent to move both X and Z forward |
| B2 channel | signal sent to move both X and Z forward |

**Table 1.** The A1 and A2 channels controlled the X piezoelectric elements correctly but the B1 and B2 channels controlling the Z sent forward signals to both the X and Z piezoelectric elements

Having checked both the connections to the hardware in the STM chamber and the connections to the control box, we determined that the problem was likely in the logic circuits inside the STM electronics box itself. Unfortunately, this was the last progress I was able to make. After I left, work on the project continued, and it was discovered that there was a broken relay in the STM control circuitry, which has now been replaced. The signals are now all correct, and both the Z and X coarse motion piezoelectric elements now operate properly.

## Project Test Scans

Several test scans were done in the process of fixing the STM scanner and checking tip heights. Figure 11 shows an uncleaned sample imaged while testing the repaired STM scanner, and Figure 12 shows an uncleaned sample imaged during the process of tip height calibration. It is possible that the low portion in Figure 12 was due to a previous tip crash on the site of the scan. Figure 11 and Figure 12 each present the data from a single scan in three different ways.

The far left frame displays the raw data from the STM scan in its original form, a top down view of the sample with color indicating the height of the STM tip as it scanned the sample's surface. The middle frame is a processed derivative image of the scan created by taking line derivatives across the topographic image. This derivative image often allows the geometry of certain features to be seen more clearly. The far right frame displays the three-dimensional topography of the sample combining aspects of the first two images. The color in the image comes from the

height information of the initial scan while the deffinition of the feature come from the derivative information shown the second image. Although this view is often less useful than the derivative image, it does give a clear sense of the sample's topography.

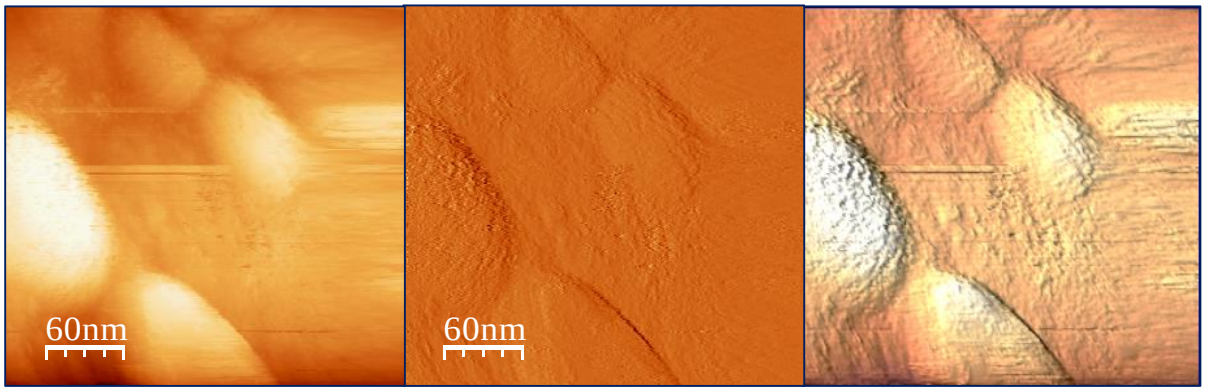


**Figure 11.** STM scan of an uncleaned sample and two processed images. At left is the raw data from the STM scan. Shown as a top view with color indicating the height of the STM tip. In the middle is a derivative image created from the processed raw data. At left is a three-dimensional image created by combining heights from the raw data with derivative information.

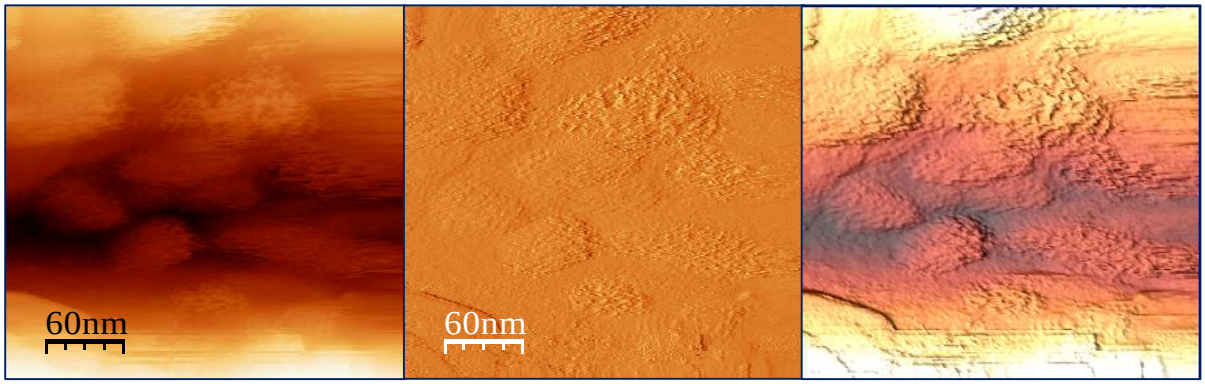


**Figure 12.** STM scan of an uncleaned sample and two processed images. At left is a top view of the raw topographic data from the STM scan. In the middle is a derivative image created from processed raw data. At right is a three-dimensional image created by combining heights from the raw data with derivative information. The unusual topography may have been created by an STM tip that had previously crashed.

WSxM STM software [6] was used to process the raw STM scan data and create both the derivative and the three-dimensional images above. Figure 13 has been included to clarify why derivative images are useful. The figure shows a cluster of pyramidal structures observed in one of van Zijll's experiments. When compared to the raw data on the left, the derivative image on

the right much more clearly shows the geometry of the pyramids with a small cap sitting on top of a rectangular base.

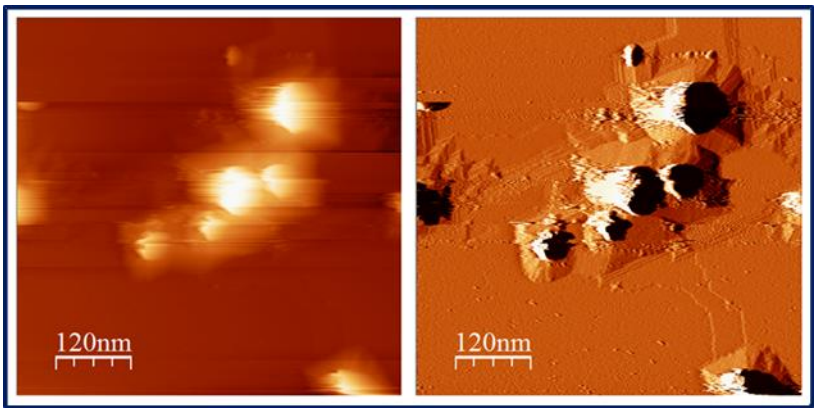


**Figure 13.** A comparison between the raw STM data and its derivative image. The derivative image emphasizes the changing heights in the scan and shows the geometry of the pyramids much more clearly. [1]

## Conclusion

Although it was not verified during the summer that the pyramidal structures that Van Zijll discovered in his research were a direct result of the sputtering process and not related to possible silver contamination from the sample holder, work is continuing on the project. Much progress was made in troubleshooting instrumentation and repairing hardware. Both STM scanners are now calibrated and fully functional, there is a ready supply of STM tips, and the X and Z piezoelectric elements for coarse tip motions of the STM scanner are now operational.

Recently, Andrew Kim obtained additional STM data that did not show pyramidal structures on samples that had been sputtered and annealed according to van Zijll's procedures. It appears that the silver contamination of the sample holder caused the nucleation sites for the sputtered formation of van Zijll pyramids.

## References


[1] van Zijll, Marshall. Ph.D. Dissertation, "*Scanning Tunneling Microscopy Studies of Ir on Ge(111), Ag on Ge(110), and the Effects of Sputtering Energy on Pyramids formed on Ge(110)"* UC Davis. (2014)

[2] Encyclopedia Britannica. "*Sputtering*" Encyclopedia Britannica Inc. Web. (2016) https://www.britannica.com/technology/sputtering

[3] G. Binnig and H. Rohrer, "*Scanning Tunneling Microscopy*", Physica B & C, Vol. 127, pages, 37-45. (1984).

[4] McIntyre, David. "*Quantum Mechanic: a Paradigms Approach*" Pearson. 192. (2012)

[5] G. Binnig, H. Rohrer, Ch. Gerber, and E. Weibel. "*Tunneling Through a Controllable Vacuum Gap*" Appl. Phys. Lett. 40, 178, (1982)

[6] Horcas, I., R. Fernández, J. M. Gómez-Rodríguez, J. Colchero, J. Gómez-Herrero, and A. M. Baro. "*WSXM: A Software for Scanning Probe Microscopy and a Tool for Nanotechnology*" Review of Scientific Instruments 78, no. 1 (January 1, 2007): 13705. doi:10.1063/1.2432410.


## Acknowledgments


I would like to thank my REU mentor Professor Shirley Chiang for all the time she spent teaching me solid state physics, explaining laboratory instrumentation, and otherwise giving me help and encouragement over the summer. I would also like to thank Bret Stenger for the time he spent helping me in the laboratory, and Andrew Kim for his excellent company, faith in my abilities, and many skills he taught me. In addition, I would also like to extend my sincere appreciation to Professor Rena Zieve who worked tirelessly to organize the excellent REU program at UC Davis and to the NSF Grant PHY-1560482 for funding my research experience over the summer.